

SUPPORTING INFORMATION

Microwave-assisted optimization of the manganese redox states for enhanced capacity and capacity retention of $\text{LiAl}_x\text{Mn}_{2-x}\text{O}_4$ ($x = 0$ and 0.3) spinel materials

Funeka P. Nkosi^{1,2}, Charl J. Jafta², Mesfin Kebede², Lukas le Roux², Mkhulu K. Mathe², and Kenneth I. Ozoemena^{*,1,2,3}

¹. *Department of Chemistry, University of Pretoria, Pretoria 0002, South Africa.*

². *Energy Materials, Materials Science and Manufacturing, Council for Scientific & Industrial Research (CSIR), Pretoria 0001, South Africa*

³. *School of Chemistry, University of the Witwatersrand, Private Bag 3, P O WITS 2050, Johannesburg, South Africa.*

A revised manuscript for *RSC Advances*

*Author to whom correspondence should be addressed: (K.I. Ozoemena): Tel.:+27128413664; Fax: +27128412135; E-mail: kozoemena@csir.co.za

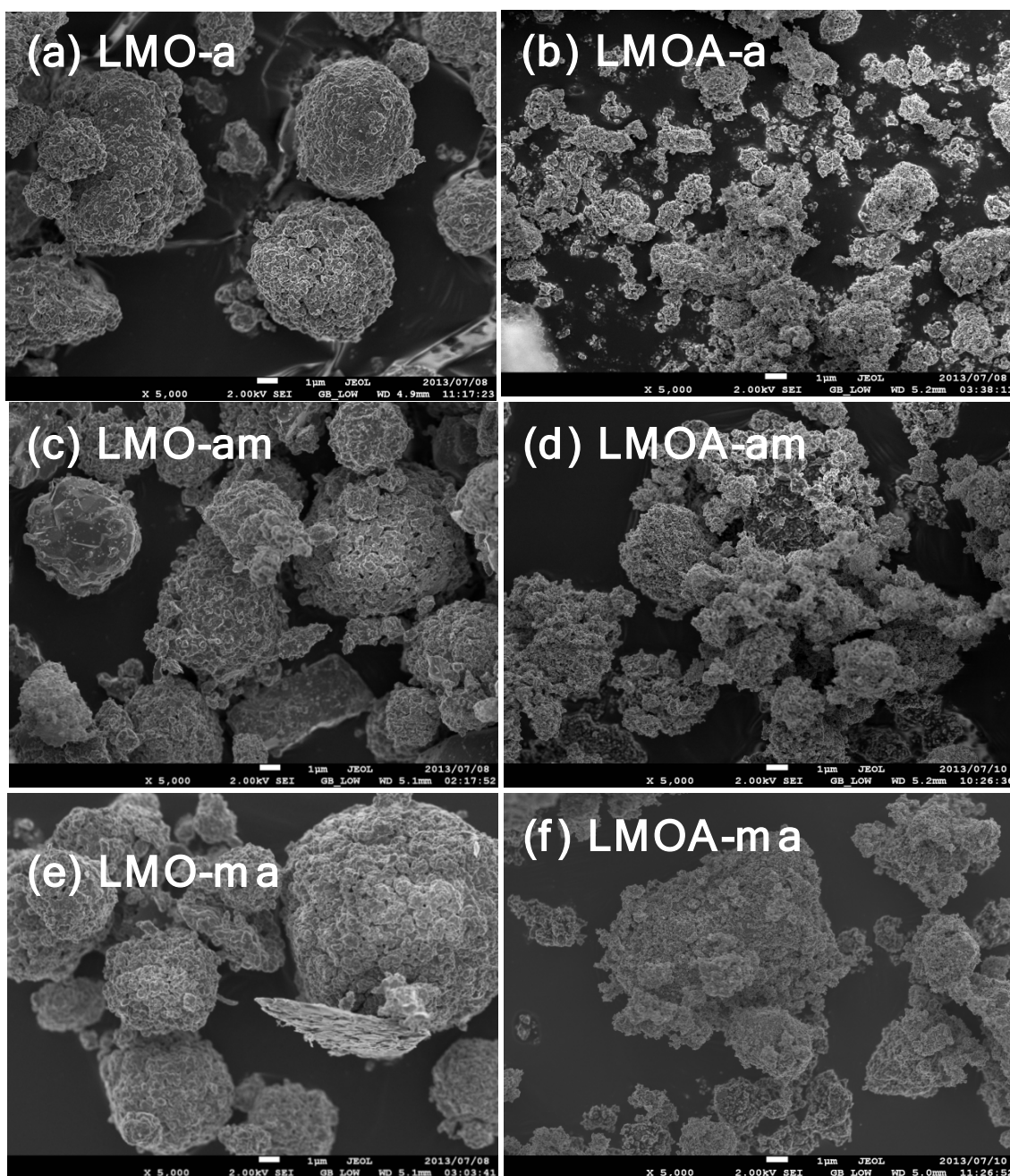


Fig. S1: Typical SEM images of LiMn_2O_4 (LMO) and $\text{LiAl}_{0.3}\text{Mn}_{1.7}\text{O}_4$ (LMOA) powders at high magnifications (1 μm). The abbreviations are as described in the main text; where symbols “a” means the materials was obtained by conventional high-temperature annealing process; “am” means that the material was subjected to microwave irradiation after obtaining

the powder by high-temperature annealing; and “**ma**” means the material was subjected to microwave irradiation prior to annealing.

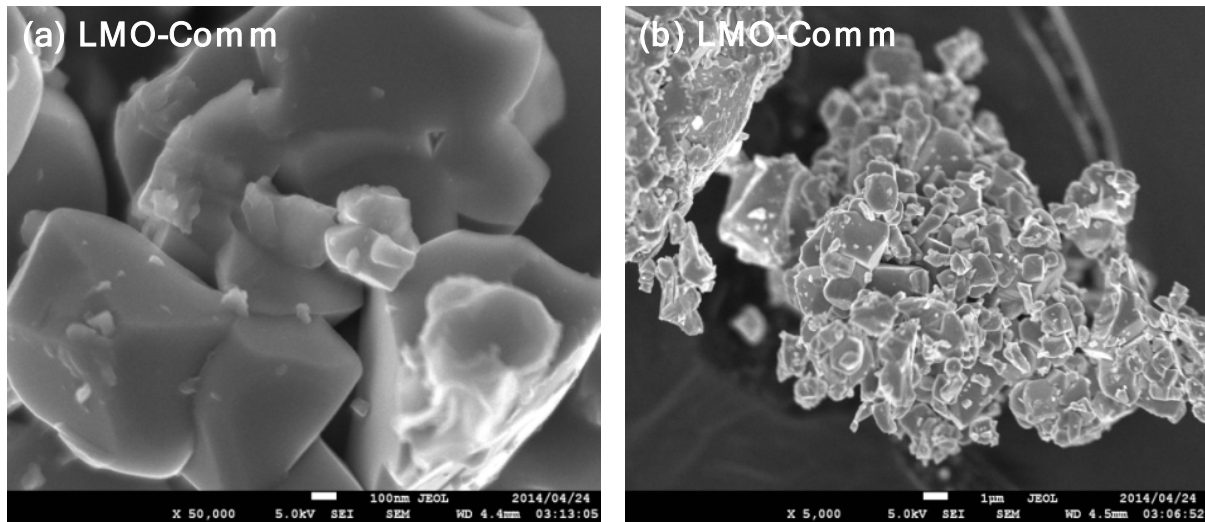


Fig. S2: SEM images of the standard commercial LMO material (LMO-comm, CAS No.: 39457-42-6, MTI Corporation, Richmond, CA., USA)

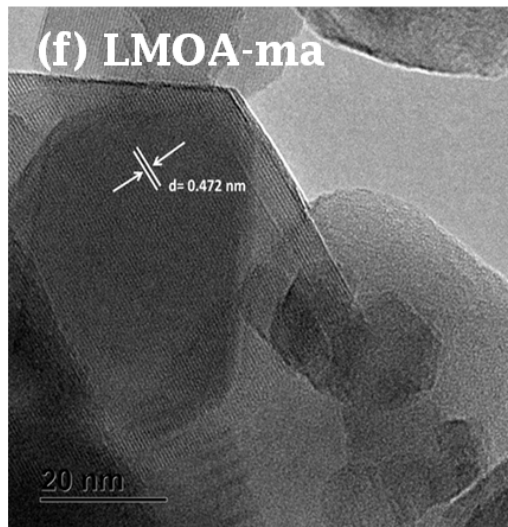
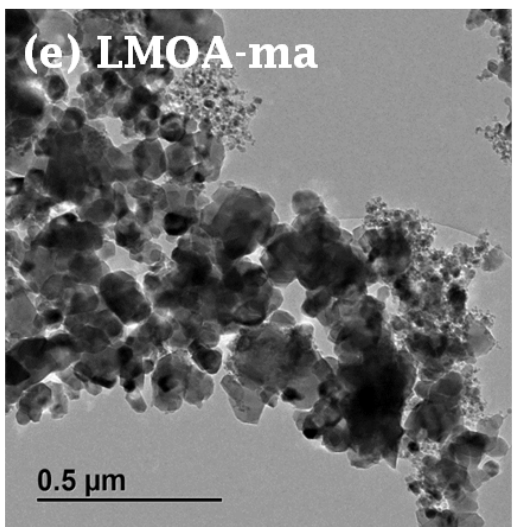
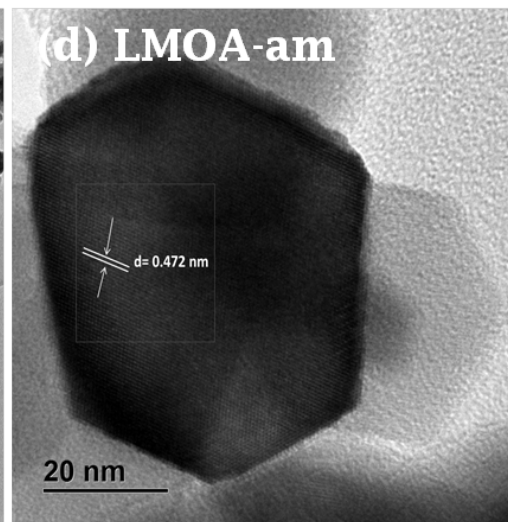
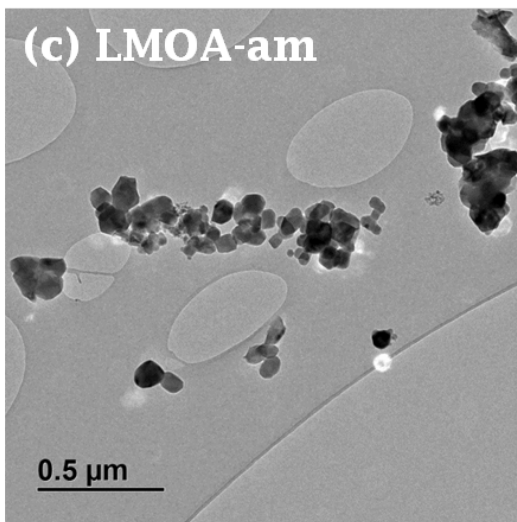
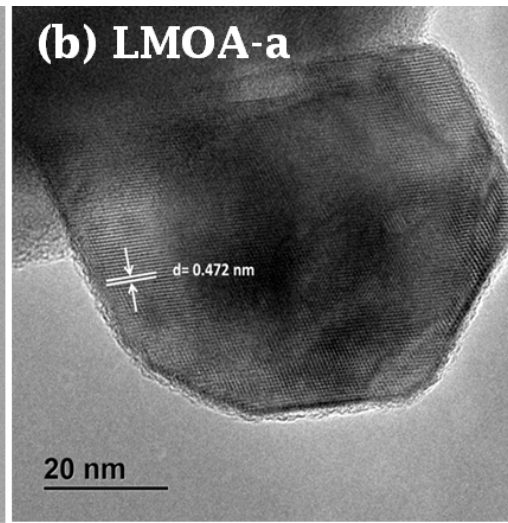
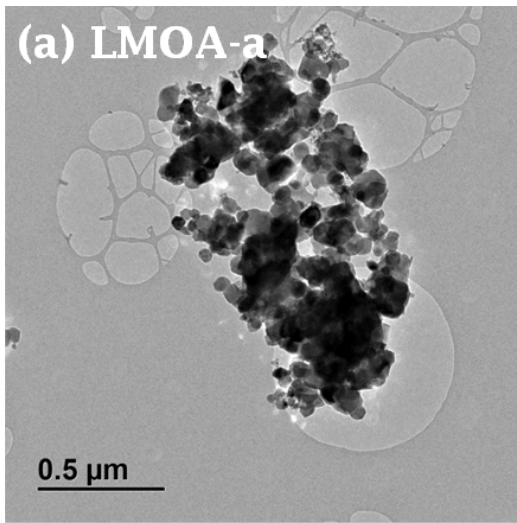


Fig. S3: Typical TEM and HRTEM images of LMOA-based powders. The abbreviations are the same as described in the main text and in *Figure S1*.

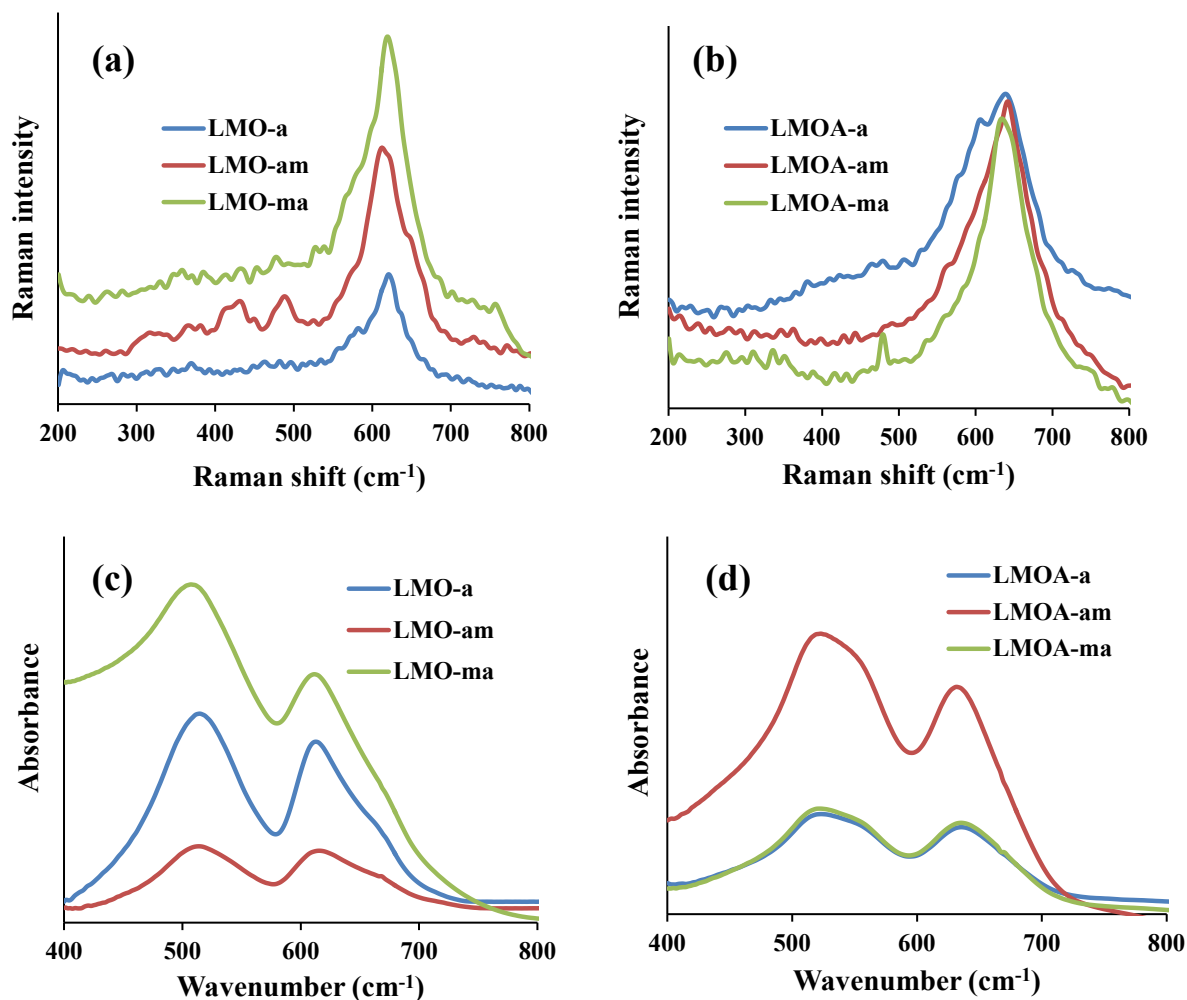


Fig. S4: Raman (a, b) and IR (c, d) spectra of the LMO- and LMOA-based spinels.

The Raman and IR spectral data (*Supporting Information, Figure S4*) are consistent with literature for LMO based spinels.¹ From the Raman spectra, the LMO samples showed pronounced peaks around 625 cm⁻¹ while the LMOA samples showed a positive shifts in the 632 – 642 cm⁻¹ range. The peaks around the 600 – 650 cm⁻¹ are due to the symmetric Mn-O stretching vibration of the MnO₆ groups, assigned to the A_{1g} species in the O_h⁷ spectroscopic

space group.² The broadening of these peaks can be attributed to the cation-anion bond lengths and polyhedral distortion occurring in LMO (i.e., the stretching vibrations of Mn^{3+}O_6 and Mn^{4+}O_6 octahedra). The positive shift of the peaks for the LMOA-based peak samples compared to the un-doped LMO is due to the existence of Al^{3+} ions in some of the octahedral sites. Mn^{4+} has a large spin orbital constant of *ca.* 138 cm^{-1} compared to Mn^{3+} with spin orbital splitting of *ca.* 90 cm^{-1} , thus the bond strength of $\text{Mn}^{4+}\text{-O}$ increases after doping with Al^{3+} ions and thus result in the peak shifts. On the other hand, the IR spectra of the samples were dominated by two intense absorption bands in the finger print regions due the presence of the F_{1u} species, with the high frequency bands ($\geq 600\text{ cm}^{-1}$) relating to the asymmetric stretching modes of MnO_6 group. The bands appeared at *ca.* $613/515$, $616/514$ and $612/507\text{ cm}^{-1}$ for LMO-A, LMO-AM and LMO-MA, respectively, and at higher wavenumbers of *ca.* $635/523$, $632/523$, and $635/522\text{ cm}^{-1}$ for LMOA-A, LMOA-AM and LMOA-MA, respectively. The LMOA samples showed positive shift in the peak positions ($\geq 20\text{ cm}^{-1}$) positive shift in the peaks for the LMOA-based spinels is related to the which indicates a relatively stronger bonding in the $\text{Mn}(\text{Al})\text{O}_6$ octahedra due to Al-doping and the microwave irradiation. The Al-O bond (512 kJmol^{-1}) is stronger than the Mn-O bond (402 kJ mol^{-1}) in the octahedron. Interestingly, it was the microwave-treated samples with $n_{\text{Mn}} \approx 3.5+$ (i.e., LMO-ma and LMOA-am) that gave the strongest Raman and IR peaks, clearly confirming the effect of the microwave irradiation in strengthening the Mn-O bonding for enhanced electrochemistry.

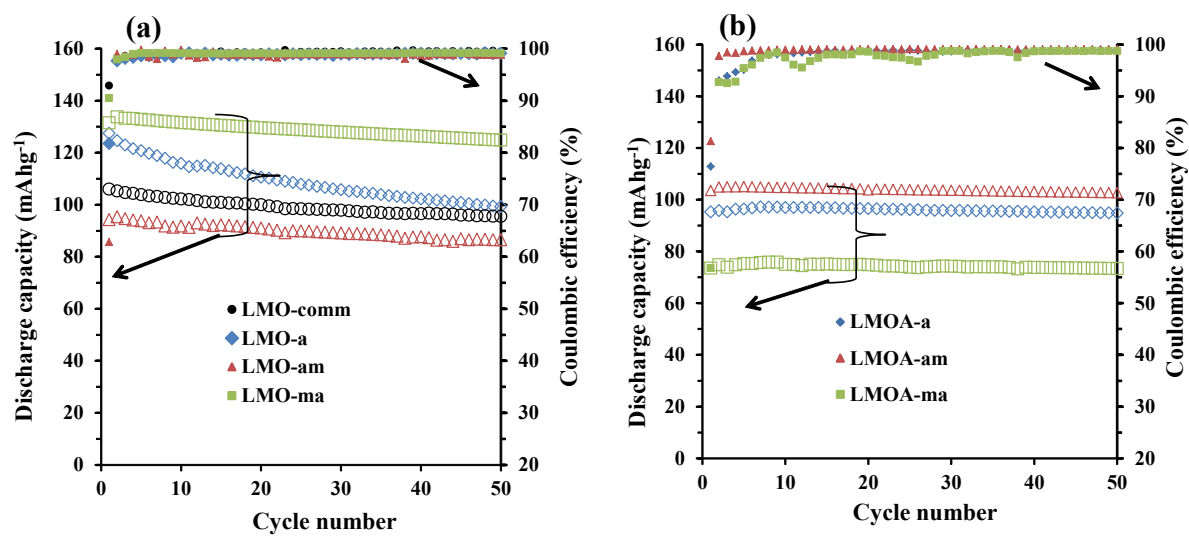


Fig. S5: Typical plots of discharge capacity vs cycle number vs coulombic efficiency for (a) LMO and (b) LMOA-based coin cell batteries.

Table S1: Cyclic voltammetric data for the redox couples shown by the LMO and LMOA-based coin cell batteries.

Material	I_{pa}/I_{pc}		ΔE_p (V)		$\Delta E_{1/2}$ (V)	
	Redox couple 1/1'	Redox couple 2/2'	Redox couple 1/1'	Redox couple 2/2'	Redox couple 1/1'	Redox couple 2/2'
LMO-a	1.06	1.22	0.16	0.12	4.00	4.13
LMO-am	1.17	1.14	0.09	0.07	4.01	4.13
LMO-ma	1.18	1.09	0.08	0.07	4.01	4.13
LMOA-a	1.07	1.50	0.10	0.13	4.00	4.14
LMOA-am	1.12	1.22	0.11	0.08	4.05	4.15
LMOA-ma	1.05	1.25	0.10	0.09	4.05	4.15

References

- 1 A. Paolone, A. Sacchetti, T. Corridoni, P. Postorino, R. Cantelli, G. Rouse and C. Masquelier, Solid State Ionics 2004, 170, 135-138.
- 2 C.M. Julien and M. Massot, Materials Science and Engineering: B, 2003, 97, 217-230.